Midgap surface bound states as signatures of possible $s^{\pm}$-wave pairing in Fe-pnictide superconductors

arXiv:1104.5282v1 [cond-mat.supr-con] 28 Apr 2011

C. S. Liu[1,2], W. C. Wu[1], and Chung-Yu Mou[3,4,5]

[1] *Department of Physics, National Taiwan Normal University, Taipei 11677, Taiwan*

[2] *Department of Physics, Yanshan University, Qinhuangdao 066004, China*

[3] *Department of Physics, National Tsing Hua University, Hsinchu 30043, Taiwan*

[4] *Institute of Physics, Academia Sinica, Nankang, Taiwan*

[5] *Physics Division, National Center for Theoretical Sciences, P.O.Box 2-131, Hsinchu, Taiwan*

(Dated: January 20, 2013)

Abstract

Appreciable zero-energy surface bound states are shown to exist in Fe-pnictide superconductors with antiphase $s^{\pm}$-wave pairing. In contrast to the [110] bound states in d-wave superconductors, these bound states arise from the non-conservation of momentum perpendicular to the interface for tunneling electrons and the $s^{\pm}$ pairing, and hence they can only exist in a small window ($\sim \pm 6^{\circ}$)in the orientation of edges near [100] direction. Our results explain why zero-bias conductance peak was often observed in tunneling spectrum and when it disappears, two coherent peaks show up, providing unambiguous signals to test the possible $s^{\pm}$-wave pairing in Fe-pnictide superconductors.

PACS numbers: 74.20.Rp,74.45.+c,74.50.+r

Recently superconductivity has been observed in several classes of Fe-pnictide materials [1–3]. One key issue towards understanding their superconductivity lies in the pairing symmetry of the Cooper pairs. A conclusive observation of the pairing symmetry remains unsettled for iron pnictides to which their superconducting (SC) gap symmetries are observed to be remarkably dependent of material classes and doping levels [4–6]. Among various candidates, the most natural and promising pairing state is considered to be the $s^{\pm}$-wave which has a sign reversal between α and β bands and can be naturally explained by the spin fluctuation mechanism [7–11].

Among phase-sensitive measurements, the point-contact Andreev-reflection spectroscopy (PCARS) is one of the high-resolution probes for detesting the SC pairing state. The zero-bias conductance peak (ZBCP) associated with Andreev bound states (ABS) in PCARS measurement has given a direct evidence on the d-wave pairing of high-T_c cuprate superconductors [12–16]. However, PCARS measurements on Fe-based superconductors has yet not yielded consistent results. Some PCARS measurements show two coherent peaks and indicate that SC pairing state might be fully gaped on the Fermi surface (FS) [17–20]. Other measurements show a ZBCP and imply the presence of zero-energy bound states or ABS on the interface [21, 22]. Moreover, depending on the direction of the sample intersurface, some PCARS has shown ZBCP coexisting with finite-energy coherent peaks [23, 24].

To address these puzzling observations, surface bound states (or midgap states) have been studied and found to appear at both zero and nonzero energies when considering the quasiparticles (QPs) interplaying between the two bands [25–27]. In fact, for a multiband system, the results of electrons tunneling and crossing the interface will be very direction dependent in terms of multiband FS topology. Moreover the existence of the surface bound states is related directly to the electron pairing potentials of different bands. Therefore a generalized theory to specifically study the possible midgap states in iron-pnictide superconductors and comparing to the PCARS measurements is in great demand. This is indeed the goal of the current paper. Here we will first show that zero-energy surface bound states exist in the possible $s^{\pm}$-wave Fe-pnictide superconductors. While for other pairing symmetries such as d-wave that support zero-energy bound states, the window of interface orientation for observing these states is usually large[16], here in contrast, we find that zero-energy bound states can exist only when the orientations of interfaces fall into a small window around $\pm 6^{\circ}$ near the [100] direction. Furthermore, off the [100] direction, the zero-bias peak disappears

and is replaced by two coherent peaks, which is due to directional dependence of QPs interplaying between different bands. These features provide unambiguous signals to test the possible $s^{\pm}$-wave pairing in Fe-pnictide superconductors.

The Model — For Fe-pnictide superconductors, the so-called α_1 and α_2 Fermi sheets are concentric and nearly circular hole pockets around the Γ point. While β_1 and β_2 Fermi sheets are nearly circular electron pockets around the M points [28–30]. High-resolution angle-resolved photoelectron spectroscopy (ARPES) measurements have been performed on superconducting $Ba_xK_{1-x}Fe_2As_2$ from under-, optimally- to over-doped samples. It was shown that SC gaps on each FS are nearly isotropic. Besides, a large gap was observed on the two small hole-like β_1 and β_2 FSs as well as on electron-like α_1 Fermi sheet, while a small gap was observed on the large hole-like α_2 FS. These FS sheets are sketched in Fig. 1. Our discussions will follow the above picture of Fermi surfaces and SC gap structures.

We first consider a Fe-pnictide bulk superconductor with a perfectly flat and infinitely large interface located at $x = 0$. For *each* band, QP states have a coupled electron-hole character and can be described by the BdG equations [31]

$$\begin{bmatrix} \hat{\xi} & \Delta(\mathbf{r}) \\ \Delta^*(\mathbf{r}) & -\hat{\xi} \end{bmatrix} \begin{bmatrix} u(\mathbf{r}) \\ v(\mathbf{r}) \end{bmatrix} = E \begin{bmatrix} u(\mathbf{r}) \\ v(\mathbf{r}) \end{bmatrix}, \tag{1}$$

where $\hat{\xi} \equiv -\hbar^2\nabla^2/2m - \mu$ with μ the chemical potential and m the electron mass. We shall seek a solution of the form

$$u(\mathbf{r}) = e^{i\mathbf{k}_F\cdot\mathbf{r}}\eta(\mathbf{r}) \quad \text{and} \quad v(\mathbf{r}) = e^{i\mathbf{k}_F\cdot\mathbf{r}}\chi(\mathbf{r}), \tag{2}$$

where $\mathbf{k}_F$ is Fermi wavevector and in contrast to the plane-wave exponential factors, $\eta(\mathbf{r})$ and $\chi(\mathbf{r})$ are slowly varying functions. Neglecting the second derivatives, we thus obtain the Andreev equations

$$\begin{aligned} &[i\hbar(\mathbf{v}_F\cdot\nabla) + E]\,\eta(\mathbf{r}) + \Delta(\mathbf{r})\,\chi(\mathbf{r}) = 0, \\ &[i\hbar(\mathbf{v}_F\cdot\nabla) - E]\,\chi(\mathbf{r}) + \Delta(\mathbf{r})\,\eta(\mathbf{r}) = 0. \end{aligned} \tag{3}$$

It is assumed that the pairing gap function takes the steplike form, $\Delta(x, y, z) = \Delta e^{i\phi}\theta(x)$. In reality, it sags a little near the interface at the distance of about the mean free path. In the following discussion, we neglect the above so-called proximity effect since it brings only small corrections. As the wave-vector components, k_y, parallel to the interface are conserved for all possible processes, the problem is effectively reduced to one-dimensional one.

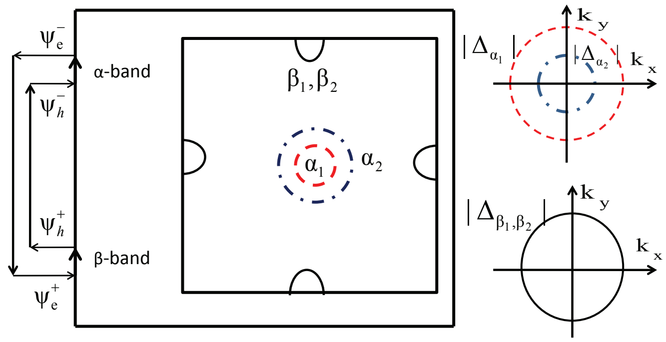

FIG. 1. (Color online) Panel (a): schematic plot of the Saint-James cycle for an Fe-pnictide two-band superconductor interface. The interface is oriented along the [100] direction. Panel (b): schematic plot of the s-wave SC gap amplitudes associated with different Fermi sheets.

The two bands are assumed to be decoupled completely and thus one can proceed to obtain various reflection coefficients for each individual band. Outside of the interface, electrons and holes, if existing, are free electrons and free holes and we denote their wave functions by $\psi^{\pm}_{e(h)}(x)$ with k_y suppressed. Here e (h) denotes for electron (hole) and $+$ ($-$) corresponds to movement parallel (antiparallel) to the x-axis. Inside of the superconductor, one can solve the Andreev equation (3) to obtain electron- and hole-like quasiparticle (QP) wave function $\Psi^{\pm}_{e(h)}(x)$.

When a free electron is injected into the interface, two possible reflections and their related coefficients are as follows: (a) normal reflection (reflected as electrons) with the coefficient r_{ee} and (b) Andreev reflection (reflected as holes, due to electron and hole coupling in the $\mathbf{k}$ subspace) with the coefficient r_{eh}. On the contrary, when a free hole is injected into the interface from the vacuum, there also exist two kinds of reflection: (a) normal reflection with the coefficient r_{hh} and (b) Andreev reflection (reflected as electrons) with the coefficient r_{he}. Matching the wave functions and their derivatives at the interface ($x = 0$), after some tedious but straightforward calculations, the Andreev reflection coefficients can be obtained to be

$$r_{eh(he)} = e^{\mp i\phi} \times \begin{cases} e^{-i \arccos \frac{E}{\Delta}}, & \text{for} \quad E \leq \Delta, \\ e^{-\mathrm{arccosh} \frac{E}{\Delta}}, & \text{for} \quad E > \Delta. \end{cases} \tag{4}$$

For the subgap (or midgag) state, $E \leq \Delta$, we thus have for the total Andreev reflection $|r_{eh(he)}(E)|^2 = 1$. The normal reflection can be generally neglected [32].

With various reflection coefficients, we are in the position to discuss the QP tunneling. Following the formulation of Hu[12], surface bound states of a Fe-pnictide superconductor can be obtained by considering QP states of a metal layer of width w attached to the interface in the limit of $w \to 0$. In this limit, the solution to the Andreev equations (3) inside the metal layer for a given k_y can be written as

$$\begin{aligned} \psi(0,E) &= a\psi_e^+(0,E) + b\psi_h^+(0,E) \\ &\quad + c\psi_e^-(0,E) + d\psi_h^-(0,E), \end{aligned} \tag{5}$$

Due to *non-conservation of momentum* perpendicular to the interface at $x = 0$ when QPs scatter off the interface, QP will scatter across α and β bands as shown in Fig. 1 for the case of $k_y = 0$: An electron in the metal layer moving towards the interface will be Andreev reflected as a hole by the pair potential in β band. This hole will then be specularly reflected at the outer (free) surface, after which it will be Andreev reflected as an electron by the pair potential in α band. This electron will then, in turn, be specularly reflected on the free surface, which will form a close Saint-James cycle [14]. Quantitatively, one decomposes wave functions into partial waves in α and β bands by writing $\psi^{\pm}_{e(h)} = \psi^{\pm}_{\alpha e(h)} + \psi^{\pm}_{\beta e(h)}$ with the following relations

$$\begin{aligned} c\psi_{\alpha e}^-(0,E) &= r_{he} d\psi_{\alpha h}^-(0,E), \\ b\psi_{\beta h}^+(0,E) &= r_{eh} a\psi_{\beta e}^+(0,E), \\ d\psi_{\alpha h}^-(0,E) &= -b\psi_{\beta h}^+(0,E), \\ a\psi_{\beta e}^+(0,E) &= -c\psi_{\alpha e}^-(0,E), \end{aligned} \tag{6}$$

where the last two equations result from the specular reflections on the free surface. Note that the reversed cycle is an equivalent cycle in which one simply exchanges α and β in (6). Clearly, Eq. (6) implies $r_{eh}(\beta)r_{he}(\alpha) = 1$ and $r_{eh}(\alpha)r_{he}(\beta) = 1$ for the reversed cycle. By using Eq. (4), we find that the midgap energy in the two-band system must satisfy

$$\begin{aligned} \arccos\frac{E_n}{\Delta_\alpha} + \arccos\frac{E_n}{\Delta_\beta} &= \pm(\phi_\alpha - \phi_\beta) + 2n\pi, \\ \text{with} \quad n &= 0, \pm 1, \cdots \end{aligned} \tag{7}$$

Eq. (7) represents one of the major results in this paper. If one identifies the scattering phase across the interface as the generalized momentum, $p_i = \pm\phi_i + \arccos\frac{E}{\Delta_i}$, Eq. (7) can be rewritten as $\sum_{i=(\alpha,\beta)} p_i = 2n\pi$, which is in consistence with the semiclassical quantization

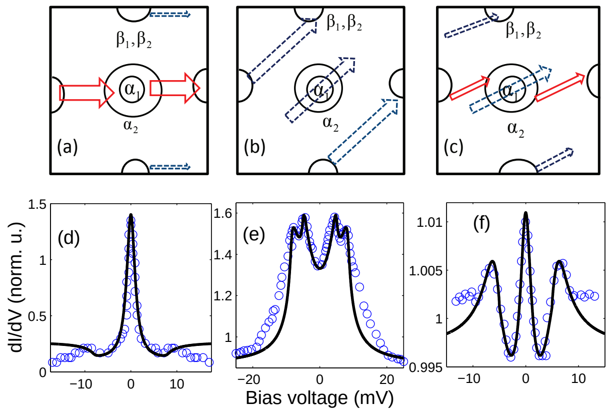

FIG. 2. (Color online) Panel (a)–(c): schematic plots of different-direction electron tunneling on iron-pnictide SC interfaces. The arrows denote the electron tunneling directions and how different bands are coupled. The arrows with red sold lines show the particular directions where zero-energy Saint-James cycle can form. The weights of the arrows denote their possible contributions to the differential conductance. Panel (d)–(f): fitting to the G-V data of (d) $SmFeAsO_{0.9}F_{0.1}$ sample ($T_c = 51.5$K) (taken from Ref. [23]); (e) $TbFeAsO_{0.9}F_{0.1}$ sample ($T_c = 50$K) (taken from Ref. [24]); and (f) $SmFeAsO_{0.9}F_{0.1}$ sample ($T_c = 51.5$K) (taken from Ref. [23]).

condition. When $\Delta\phi = \phi_\alpha - \phi_\beta = \pm\pi$ and $E_n < \Delta_\alpha < \Delta_\beta$, Eq. (7) only supports the zero-energy solution ($E_n = 0$). It indicates that zero-energy surface bound states exist in the semiclassical approximation. Furthermore, since both Saint-James cycle and its reversed cycle support zero-energy state, there will be two non-dissipative currents associated with the zero-energy states. It should be noted that no Saint-James cycle exists when $\Delta_\alpha < E_n < \Delta_\beta$ or $\Delta_\alpha < \Delta_\beta < E_n$ because according to Eq. (4), the currents will decay exponentially.

Results and Discussions – To consider how the above midgap states are related to real PCARS measurements, we extend the above analysis to cases with $k_y \neq 0$ in the following. If the pairing gaps between different FSs are extended s-wave with sign reversal, there will be four kinds of zero-energy surface bound states (or zero-energy Saint-James cycles) corresponding to various combinations of interband FSs: $\alpha_1 - \beta_1$, $\alpha_1 - \beta_2$, $\alpha_2 - \beta_1$, and $\alpha_2 - \beta_2$. In addition to the above four zero-energy surface bound states, there also exist nonzero-energy surface bound states (or nonzero-energy Saint-James cycles) corresponding to various combinations of intraband FSs: $\alpha_1 - \alpha_1$, $\alpha_2 - \alpha_2$, $\beta_1 - \beta_1$, and $\beta_2 - \beta_2$.

To extend our analysis to investigate PCARS, the metal layer is replaced by a metal tip

occupying $x < 0$. When an electron is injected into the interface from the tip, there occur two possible reflections: (i) normal reflection (reflected as electrons) with the coefficient r_N and (ii) Andreev reflection (reflected as holes) with the coefficient r_A. In terms of r_N and r_A, the resulting wave function for the normal side ($x < 0$) can be written as $\Psi_N = \psi_e^+ + r_N\psi_e^- + r_A\psi_h^+$. On the SC side, for the zero-energy Saint-James cycle, the transmitted electron-like and hole-like QPs are mainly in different bands, experiencing different pairing potentials for $s^{\pm}$-wave Fe-pnictide superconductors. We shall take the electron-like QP to be in the α bands. The corresponding wave function Ψ_e^+ is obtained by solving the Andreev equation (3) with pairing potential $\Delta_\alpha e^{i\phi_\alpha}$. Similarly, the hole-like QP wave function Ψ_h^+ can be obtained by solving the Andreev equation (3) with pairing potential $\Delta_\beta e^{i\phi_\beta}$. Superposition of the two eigenstates, Ψ_e^+ and Ψ_h^+, will give a resulting wave function $\Psi_S = c_1\Psi_e^+ + c_2\Psi_h^+$ for the SC side. Matching the wave functions and their derivatives at the interface $x = 0$, the normal reflection amplitude r_N and the Andreev reflection amplitude r_A can be found [13]. Similar calculations apply to non-zero Saint-James cycles. From the knowledge of r_N and r_A, the normalized differential conductance dI/dV is found according to the formula $\sigma_S = 1 + |r_A|^2 - |r_N|^2$[32].

When the interface is along the [100] direction as shown in Fig. 1 or Fig. 2(a), the dominant contribution to the current comes from electrons with $k_y \sim 0$, i.e., most electrons tunnel normal to the interface. Due to non-conservation of k_x, QPs will scatter into different bands. The low-energy differential conductance will thus be dominated by the zero-energy bound states arising from the interband QP transitions although the nonzero-energy bound states may also have some effects on it. Thus the ZBCP found in PCARS is due to the zero-energy bound states that exist in the interface when electrons are tunneled normal to the interface along the [100] direction. This is verified in Fig. 2(d), where we have simulated the PCARS data presented in Ref. [23] by assuming that all electrons are tunneling across the interface along the [100]-direction. The best fitting is obtained with $\Delta_\alpha = 8$ and $\Delta_\beta = 8$ under the proposed sign-reversal $s^{\pm}$-wave pairing. The normalized barrier height is taken to be $Z = 5$ and the scattering broadening $\Gamma = 0.5$. It should be emphasized that the ZBCP is more sensitive to the phase difference than the gap amplitude and when a more realistic FS together with a more realistic extended s-wave gap are used, a much better fitting, especially in the nonzero-energy region, will be obtained. The ZBCP found here can only exist when range of k_y covers the β band. Using experimental data[29, 30], this corresponds to a small

window of $\pm 6°$ for interfaces around [100] direction.

We next consider the case when the interface is off the window of $\pm 6°$ about [100]. In Fig. 2(b), we consider tunneling in the [110] direction with corresponding range of k_y. The directional detuning results in the absence of ZBCP. However, we found that the differential conductance is dominated by the nonzero-energy bound states due to intraband QP transitions. This is the key why two coherent peaks are often observed in the PCARS measurements. In Fig. 2(e), we use the two-gap $s^{\pm}$-wave model to fit the PCARS data reported in Ref. [24]. The best fitting was obtained with the two gap amplitudes set to $\Delta_\alpha = 8.5$ and $\Delta_\beta = 5$. The broadening is taken to be $\Gamma = 0.5$.

In Fig. 2(c), we consider the case when the orientation of the interface is between [100] and [110] but falls into the window of $\pm 6°$ about [100]. In such case, both nonzero- and zero-energy bound states are equally important to the differential conductances and ZBCP is often observed due to zero-energy midgap state. Moreover, when electrons tunnel into the superconductor across the interface, QPs from different bands are coupled. Due to different gap amplitudes on different FSs and finite QP life time, one effective gap amplitude can be generally observed in experiment. In Fig. 2(f), we have used one gap amplitude sign reversal [as done in Fig. 2(a)] to fit the PCARS data [23]. For the best fitting, the effective gap amplitude is taken to be $\overline{\Delta} = 6.5$ with broadening being $\Gamma = 1.5$, while the sign-change gap amplitude is taken to be $\Delta = 5$ with the broadening being $\Gamma = 0.01$.

In summary, we have investigated signatures of antiphase $s^{\pm}$-wave pairing in Fe-pnictide superconductors due to zero-energy surface bound states. It is found that while for other pairing symmetries such as d-wave that support zero-energy bound states, the window of interface orientation for observing these states is usually large, for $s^{\pm}$-wave, however, zero-energy bound states can exist only when the orientations of interfaces fall into a small window around $\pm 6°$ near the [100] direction. Off the [100] direction, the zero-bias peak disappears and is replaced by two coherent peaks, due to directional dependence of QPs interplaying between different bands. Our results give a unified explanation to the PCARS experimental data in various directions and indicate strongly that the pairing of Fe-pnictide superconductors is the $s^{\pm}$-wave in different bands.

This work was supported by National Science Council of Taiwan (Grant Nos. 100-2811-M-007-015 and 99-2112-M-003-006), Hebei Provincial Natural Science Foundation of China (Grant No. A2010001116), and the National Natural Science Foundation of China (Grant

No. 10974169). We also acknowledge the support from the National Center for Theoretical Sciences, Taiwan.

[1] Y. Kamihara *et al.*, J. Am. Chem. Soc. **130**, 3296 (2008).

[2] X. H. Chen *et al.*, Nature **453**, 761 (2008).

[3] F.-C. Hsu *et al.*, Proc. Natl. Acad. Sci. **105**, 14262 (2008).

[4] C. W. Hicks *et al.*, Phys. Rev. Lett. **103**, 127003 (2009).

[5] H.-J. Grafe *et al.*, Phys. Rev. Lett. **101**, 047003 (2008).

[6] K. Hashimoto *et al.*, Phys. Rev. Lett. **102**, 017002 (2009).

[7] Z. J. Yao, J. X. Li, and Z. D. Wang, New Journal of Physics **11**, 025009 (2009).

[8] I. I. Mazin, D. J. Singh, M. D. Johannes, and M. H. Du, Phys. Rev. Lett. **101**, 057003 (2008).

[9] F. Wang *et al.*, Phys. Rev. Lett. **102**, 047005 (2009).

[10] F. Wang, H. Zhai, and D.-H. Lee, Phys. Rev. B **81**, 184512 (2010).

[11] M. B. K. Z.-A. R. . Z. X. Z. C.-T. Chen, C. C. Tsuei, Nature Physics **6**, 260 (2010).

[12] C.-R. Hu, Phys. Rev. Lett. **72**, 1526 (1994).

[13] Y. Tanaka and S. Kashiwaya, Phys. Rev. Lett. **74**, 3451 (1995).

[14] G. Deutscher, Rev. Mod. Phys. **77**, 109 (2005).

[15] S. T. Wu and C. Y. Mou, Phys. Rev. B **66**, 012512 (2002).

[16] S. T. Wu and C. Y. Mou, Phys. Rev. B **67**, 027503 (2003).

[17] L. Shan *et al.*, EPL **83**, 57004 (2008).

[18] P. Szabó *et al.*, Phys. Rev. B **79**, 012503 (2009).

[19] M. Tortello *et al.*, Phys. Rev. Lett. **105**, 237002 (2010).

[20] M. Tortello *et al.*, Journal of Superconductivity and Novel Magnetism **22**, 553 (2009).

[21] K. A. Yates *et al.*, Superconductor Science and Technology **21**, 092003 (2008).

[22] X. Lu *et al.*, Superconductor Science and Technology **23**, 054009 (2010).

[23] Y.-L. Wang *et al.*, Superconductor Science and Technology **22**, 015018 (2009).

[24] K. A. Yates *et al.*, New Journal of Physics **11**, 025015 (2009).

[25] A. A. Golubov, A. Brinkman, Y. Tanaka, I. I. Mazin, and O. V. Dolgov, Phys. Rev. Lett. **103**, 077003 (2009).

[26] P. Ghaemi, F. Wang, and A. Vishwanath, Phys. Rev. Lett. **102**, 157002 (2009).

[27] D. Wang, Y. Wan, and Q.-H. Wang, Phys. Rev. Lett. **102**, 197004 (2009).

[28] D. J. Singh and M.-H. Du, Phys. Rev. Lett. **100**, 237003 (2008).

[29] H. Ding *et al.*, EPL **83**, 47001 (2008).

[30] K. Nakayama *et al.*, Phys. Rev. B **83**, 020501 (2011).

[31] P. G. de Gennes, *Superconductivity of Metals and Alloys* (Benjamin, New York, 1996).

[32] G. E. Blonder, M. Tinkham, and T. M. Klapwijk, Phys. Rev. B **25**, 4515 (1982).